Communications

Mode-Dependent Fano Resonances Observed in the Predissociation of Diazirine in the S_1 State**

Doo-Sik Ahn, So-Yeon Kim, Goo-Il Lim, Sungyul Lee,* Young S. Choi,* and Sang Kyu Kim*

Resonance in chemical reactions is a very intriguing quantum mechanical phenomenon and provides essential information about the detailed shape of the potential-energy surfaces especially near the nuclear configuration that is critical for dynamical constraints.[1] Fano-type resonance is particularly interesting since it results from the interference of two distinct reactive pathways leading to the same product channel.[2] When an atom is excited to a super-excited state above the ionization threshold energy, and for instance, the isoenergetic continuum is coherently excited at the same time, this results in the interference of direct and indirect ionization processes to give the asymmetric line shape in the ionization cross section.[3] Fano resonance has often been found in the ionization cross section of atoms, whereas its observation in the molecular systems is very rare, especially in gas-phase dynamics. Only a few cases have been reported to date in vibrational autoionization of H_3[4] or predissociation of H_2,[5] Cs_2,[6] and FNO.[7] The multidimensionality of the internal coordinate of polyatomic molecules generally makes the observation of the Fano resonance more difficult since the coherent excitation of bound and continuum states is less probable when the number of internal degrees of freedom increases. The intrinsic spectral congestion of polyatomic molecules may also hamper the experimental observation of asymmetric resonance. Consequently, Fano resonances in polyatomic systems have rarely been interrogated in chemical reactions. Herein, we report the observation of Fano profiles in the partial photodissociation cross section of the diazirine. The yield of the nascent $^1CH_2(\tilde{B})$ fragment from the S_1 state of diazirine has been monitored as a function of the excitation energy by detecting the total fluorescence emitting in the $^1CH_2(\tilde{B})$ to $^1CH_2(\tilde{A})$ transition. All of the Franck–Condon active bands show asymmetric line shapes, giving the mode-dependent dynamic parameters, such as homogeneous line width, center of resonance frequency, and the asymmetry parameter. The symmetric and asymmetric C−N stretching modes exhibit quite different Fano profiles, giving qualitative and yet essential information about the shape of the potential-energy surface in the vicinity of the transition state. Especially since the interference in the reaction pathways could be further utilized to control the outcomes of chemical reactions,[7] the experimental finding of the Fano resonance in a polyatomic molecule may open the possibility of controlling the reaction of complicated molecular systems in multidimensional coordinates through the manipulation of the phase involved in the excitation process.

Diazirine (CH_2N_2), as a clean source of carbene and a precursor of diazomethane,[8] has been intensively studied theoretically. However because of the lack of experimental studies, even the structure and dephasing mechanism of diazirine in the first electronically excited state (S_1) are still the subject of controversy.[9] The only molecular-beam experimental work on diazirine (S_1) is the report that the excited singlet state of methylene, $^1CH_2(\tilde{B})$, is produced from the S_1–S_0 origin band of diazirine.[10]

In our current investigation, the total emission from $^1CH_2(\tilde{B})$ was monitored as a function of the pump energy to give the photofragment excitation (PHOFEX) spectrum for the S_1–S_0 transition of diazirine. The PHOFEX signal reflects the energy-dependent absorption cross section multiplied by the yield of the $^1CH_2(\tilde{B})$ fragment, representing the partial reaction cross section. The S_1–S_0 spectral origin was found at 30 967 cm^{-1}, Figure 1. All the spectral bands are found to be broad and a series of the progression bands with a fundamental frequency of 802 cm^{-1} is strongly observed. Remarkably, all the S_1 vibronic bands show asymmetric line shapes, indicating that quantum interferences should be involved in the reaction pathway leading to the generation of $^1CH_2(\tilde{B})$. The asymmetric line shape most likely indicates that the bound and continuum states are coherently excited in the S_1–S_0 transition. Therefore, the Fano profile function is used for the reproduction of the experiment is given by Equation (1), see Figure 1.[2a]

[*] Dr. D.-S. Ahn, S.-Y. Kim, Prof. S. K. Kim
Department of Chemistry and KI for Nanocentury, KAIST
Daejeon 301-750 (Korea)
Fax: (+82) 42-350-2883
E-mail: sangkyukim@kaist.ac.kr

S.-Y. Kim, Prof. S. Lee
Department of Applied Chemistry, Kyunghee University
Kyungki-Do 449-701 (Korea)
Fax: (+82) 31-202-7337
E-mail: sylee@khu.ac.kr

G.-I. Lim, Prof. Y. S. Choi
Department of Chemistry, Inha University
Incheon 402-751 (Korea)
Fax: (+82) 32-867-5604
E-mail: yschoi@inha.ac.kr

$$\sigma = \sigma' + \sigma_0(q+\varepsilon)^2/(1+\varepsilon^2),$$
$$\text{where } q = \langle b|\mu|i\rangle/(\langle c|\mu|i\rangle\pi\langle c|H'|b\rangle) \qquad (1)$$
$$\text{and } \varepsilon = 2(E-E')/\Gamma$$
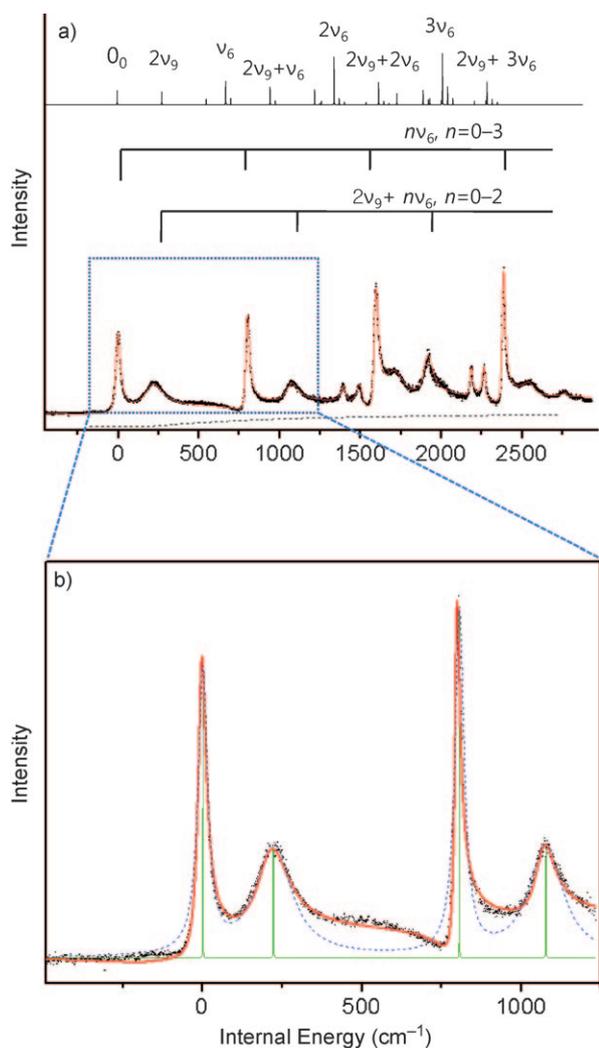
Figure 1. a) PHOFEX spectrum of diazirine with the simulation (red solid line) using the parameters listed in Table 1. Frank–Condon simulation with spectral assignments is shown above the spectrum while the σ' curve used in the Fano simulation is given beneath the spectrum (dotted line; see text for details). b) Extended view of the PHOFEX spectrum showing the simulation of the asymmetric rotor at $T_{rot} = 10$ K (green stick), the simulation convoluted by Lorentzians (blue dotted line), and Fano simulation (red solid line).

Table 1: Mode-dependent Fano-fitting parameters with band assignments.

Peaks[a] [cm^{-1}]	Calcd[b] [cm^{-1}]	Fano parameters (E',q,Γ)[c]			Assignment[d]
$T_e =$ 30967	$T_e =$ 31407	E' $T_e = 30965$	q	Γ	
0	0	0	8.0	29	0_0
216	281	213	8.0	134	$2\nu_9$
802	684	799	4.5	21	ν_6
1072	965	1072	6.0	90	$2\nu_9 + \nu_6$
1392	1508	1399	−7.7	32	ν_4
1493	1765	1499	−7.3	36	ν_3
1593	1368	1595	4.1	26	$2\nu_6$
1711	1401	1709	8.0	120	$2\nu_9 + \nu_6$[e]
1913	1649	1913	5.5	66	$2\nu_9 + 2\nu_6$
2186	2192	2186	7.0	14	$\nu_4 + \nu_6$
2265	2449	2265	−6.5	14	$\nu_3 + \nu_6$
2386	2052	2389	5.0	16	$3\nu_6$
2548	2085	2553	−4.4	80	$2\nu_8 + 2\nu_6$[e]

[a] peak values. [b] CASSCF/6-31 + G(d,p). [c] E',Γ [cm^{-1}]. [d] ν_9: C−N asymmetric stretch, ν_8: CH$_2$ torsion, ν_6: C−N symmetric stretch, ν_3: N−N stretch. ν_4: CH$_2$ deformation. [e] tentative assignments.

optical excitation process. It should be noted that there is no significant background signal in the PHOFEX spectrum, suggesting that there is little chance for the continuum electronic state to exist near the optically active $S_1(n\pi^*)$ state. The continuum character in the optical excitation should then originate from the transition-state or repulsive part of the potential-energy surface within the Frank–Condon window.

Ab initio calculations have been carried out to find the minimum-energy structure of S_1 and the associated harmonic vibrational frequencies (see Supporting Information). In the S_1 minimum energy, two C−N bonds are elongated while maintaining the C_{2v} symmetry according to the CASSCF calculation using the basis set of 6-31 + G(d,p). The vibronic band assignment is quite straightforward as listed in Table 1. The Frank–Condon simulation based on the calculated equilibrium structures of S_0 and S_1 gives a good explanation for the overall pattern of the PHOFEX spectrum, Figure 1. The C−N bond is calculated to be elongated to 1.65 Å in the S_1 energy-minimum structure compared to 1.50 Å in the S_0 equilibrium state (see Supporting Information). This large structural change upon the S_1–S_0 excitation should be responsible for the long progression of the 802 cm^{-1} band which corresponds to the symmetric C−N stretching mode (ν_6), Table 1. Since the asymmetric C−N stretching mode (ν_9) belongs to b_2, only the overtone is symmetry allowed to give the 216 cm^{-1} band. Combination bands of $n\nu_6 + 2\nu_9$ ($n = 0$–3) are then clearly identified. Weakly observed bands at 1392 and 1493 cm^{-1} are assigned to CH$_2$ deformation (ν_4) and N=N stretching (ν_3) modes, respectively. The combination bands of $\nu_6 + \nu_4$ and $\nu_6 + \nu_3$ are found at 2186 and 2265 cm^{-1}, respectively. The Fermi interaction involved in these two bands might be responsible for the q reversal observed (Table 1). The broad S_1 origin band has a line width of 29 cm^{-1}, which from a simple uncertainty formulae of $\Delta E \Delta t \approx \hbar$, gives the lifetime of approximately 200 fs. The $2\nu_9$ band at 216 cm^{-1} is found to be even broader, giving the lifetime of approximately 50 fs. These mode-dependent ultrashort lifetimes

The terms σ' or σ_0 are the cross section for direct excitation to the continuum or to the bound state, respectively. E is the excitation energy, E' represents the center of the absorption, and Γ is the line width. The q value is the asymmetry parameter and $|i\rangle$, $|b\rangle$, or $|c\rangle$ represent the initial, bound, or continuum wavefunction, respectively. μ is the transition dipole moment and H' is the coupling Hamiltonian. The Fano fit using parameters listed in Table 1 reproduces the experiment very well (Figure 1). It should be noted that the line shape should be the convolution of Fano profiles and the rotational contour associated with the $S_1(^1B_1)$–$S_0(^1A_1)$ C-type transition in the C_{2v} point group. The dynamic parameters, however, are little changed by the inclusion of the rotational distribution. The low $|q|$ values in the range of 4–8 indicate that the contribution of the direct excitation to the continuum is quite significant in the S_1–S_0

already indicate that the quantum states in the S_1 diazirine are quasi-bound in a very shallow well, and the asymmetric C−N stretching mode (v_9) should be strongly coupled to the reaction coordinate for the ring opening of diazirine leading to the excited diazomethane. It should be noted that the broad band width could also be partially ascribed to the phase space distribution of the ground-state wavefunction according to the reflection principle.[1] The strong mode dependence, however, suggests that the lifetime broadening may be dominant in the energy region studied, though for further clarification it would be highly desirable to know the detailed shape of the multidimensional potential-energy surface.

Internal conversion or a synchronous two C−N bond dissociation channel ($CH_2N_2 \rightarrow :CH_2 + N_2$) would be facilitated by the symmetric C−N stretching mode excitation if either of these were dominant dephasing process. The lower lying triplet state (T_1), because of its weak coupling strength to S_1,[9d] seems to play a minor role in the predissociation of diazirine. Thus, the ring-opening reaction is most likely to be the dominant S_1 dephasing process. Diazomethane in the excited state then undergoes the fast bond dissociation to liberate N_2 and CH_2 as final fragments. Both Ã and B̃ states of the $^1CH_2$ fragment are expected to be generated from the excited state of diazomethane, though the detailed mechanism is not the subject of the present work. The transition state for the ring-opening reaction is calculated to show the breakages of the C_2 axis and C_s plane with an imaginary frequency for the coupled motion of asymmetric C−N bond elongation and torsion of the CH_2 moiety. The transition-state structure is near the S_1 equilibrium structure and the barrier is calculated to be very low ($V_b \approx 1.2$ kJ mol^{-1}). The potential-energy surface (PES) in the vicinity of the transition state is expected to be quite flat. This situation results in a Fanck–Condon window in the S_1–S_0 optical excitation which is wide enough to cover both quasi-bound and continuum states at the same time (Figure 2). The nature of the small barrier, therefore, seems to be "dynamic" and quite subtle in this case since both direct and indirect pathways coexist, meaning that the transition state may be loosely defined. In the time-dependent picture, the initial wave packet bifurcates into two distinct pathways, one of which is direct whereas the other is rather indirect with some recurrences.[7] This bifurcation occurs for all vibronic bands showing asymmetric Fano profiles while the mode-dependent dynamic barrier might exist depending on the extent of coupling to the reaction coordinate. Along the modes perpendicular to the reaction coordinate, the vibrational adiabaticity seems to be maintained. For instance, the $v_6 = 1$ band is found to be slightly sharper than the zero-point-energy band even though the excitation energy of the $v_6 = 1$ band is higher than the zero-point-energy band. More interestingly, the natural lifetime associated with the combination band of $v_6 + 2v_9$ is longer than that of the $2v_9$ band, suggesting that the $2v_9$ excited level may experience a slightly higher effective dynamic barrier when the symmetric C−N stretching mode (v_6) is combined. This-mode dependent lifetime strongly indicates that the reactive flux follows the adiabatic path along which the vibrational mode perpendicular to the reaction coordinate may act as an observer during the passage of the reactive flux.
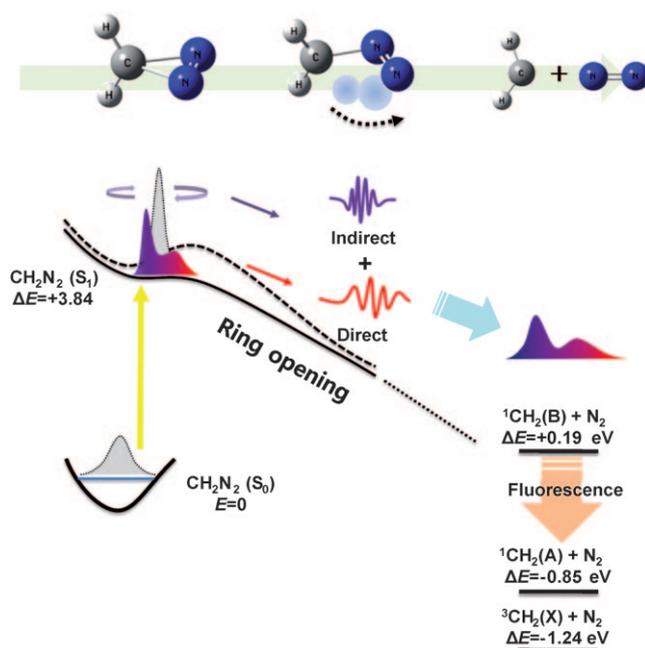
Figure 2. Schematic diagram showing the excitation of the bound and transition-state regions of the S_1 diazirine. The broken line represents a typical vibrational adiabatic surface showing a dynamic barrier, the nature of which depends on the extent of coupling to the reaction coordinate.

The v_3 (N=N stretching) and v_4 (CH_2 deformation) bands are also explainable by the same scenario. Namely, since those modes are much less coupled to the reaction coordinate, more recurrences take place prior to the ring-opening reaction giving the relatively sharper spectral features (Figure 1 and Table 1). It is also noteworthy that two bands observed at 1711 and 2548 cm^{-1}, which are tentatively assigned to $v_6 + 2v_8$ and $2v_6 + 2v_8$, respectively, may indicate that the torsional motion of the CH_2 moiety (v_8) is involved in the reaction coordinate. Another point is that the production of the $^1CH_2$(B̃) fragment from diazirine requires the breakage of two equivalent C−N bonds, and whether these two bonds break in a concerted or stepwise manner is an interesting dynamic issue. In the case of diazirine in S_1, according to our experiment, two bond-breaking events seem to occur in a stepwise manner.

In conclusion, Fano-type resonances in the predissociation of the five-atom molecule diazirine have been observed for the first time. As a result of the multidimensionality of the potential-energy surfaces, the mode effect of the Fano resonances gives crucial information about the detailed shape of the potential-energy surface in the vicinity of the Franck–Condon accessed transition state. The asymmetric C−N stretching mode is found to be most strongly coupled to the reaction coordinate for the S_1 dephasing process, and the S_1 dephasing process corresponds to the ring-opening reaction that leads to excited diazomethane, finally giving $^1CH_2$(B̃) + N_2 as one of the product channels. It is remarkable that mode-dependent Fano resonances could resolve many key issues of the complicated predissociation dynamics of the excited diazirine quite clearly. Product-state distribution and time-

resolved dynamic studies would be quite helpful for further unraveling the whole reaction pathway from diazirine (through diazomethane) to nitrogen and methylene radical. The Fano resonances in polyatomic molecular systems observed in this work give the opportunity to disentangle the complicated dynamics occurring on the excited state even without the complete calculation of the potential-energy surfaces. Deep insights into the morphology of the potential-energy surface near the transition state have been invoked from the analysis of quantum-mechanical interferences and therefore this work provides the unique opportunity to control the outcome of chemical reactions by phase manipulation.

Experimental Section

Diazirine was synthesized according to the procedure described in Ref. [8]. The detailed experimental setup had been described in our previous publication.[10] The premixed diazirine/He gas (3%, 1 atm) was expanded into vacuum through 0.5 mm diameter nozzle to generate the molecular beam. The fluorescence signal from $^1CH_2(\tilde{B})$ was identified by measuring the intrinsic lifetime and spectral characteristic. All ab initio calculations were implemented with the quantum chemical programs (Gaussian03,[11] ACESII[12] and Molpro[13]). The active space for the CASSCF calculation was performed with six electrons on six active orbitals. The Frank–Condon integral calculation was carried out with MolFC program[14] based on the Duchinsky matrix approximation.

[1] a) R. Schinke, *Photodissociation dynamics*, Cambridge University Press, Cambridge, **1993**; b) R. N. Zare, *Science* **2006**, *311*, 1383.

[2] a) U. Fano, *Phys. Rev.* **1961**, *124*; b) S. Y. Lee, *J. Chem. Phys.* **1995**, *103*, 3501; c) S. Lee, *Bull. Korean Chem. Soc.* **2000**, *21*, 331.

[3] S. Tauro, K. P. Liu, *J. Phys. B* **2008**, *41*.

[4] M. C. Bordas, L. J. Lembo, H. Helm, *Phys. Rev. A* **1991**, *44*, 1817.

[5] P. M. Dehmer, W. A. Chupka, *J. Chem. Phys.* **1976**, *65*, 2243.

[6] B. Kim, K. Yoshihara, S. Lee, *Phys. Rev. Lett.* **1994**, *73*, 424.

[7] a) J. T. Brandon, S. A. Reid, D. C. Robie, H. Reisler, *J. Chem. Phys.* **1992**, *97*, 5246; b) R. Cotting, J. R. Huber, V. Engel, *J. Chem. Phys.* **1994**, *100*, 1040; c) S. A. Reid, J. T. Brandon, H. Reisler, *J. Phys. Chem.* **1993**, *97*, 540; d) H. U. Suter, J. R. Huber, M. V. Dirke, A. Untch, R. Schinke, *J. Chem. Phys.* **1992**, *96*, 6727.

[8] a) E. S. Schmitz, R. Ohme, *Tetrahedron Lett.* **1961**, *2*, 612; b) S. R. Paulson, *Angew. Chem.* **1960**, *72*.

[9] a) M. J. Amrich, J. A. Bell, *J. Am. Chem. Soc.* **1964**, *86*, 292; b) B. Bigot, R. Ponec, A. Sevin, A. Deavaquet, *J. Am. Chem. Soc.* **1978**, *100*, 6575; c) P. L. Mueller-Rammers, K. Jug, *J. Am. Chem. Soc.* **1985**, *107*, 7275; d) N. Yamamoto, F. Bernardi, A. Bottoni, M. Olivucci, M. A. Robb, S. Wilsey, *J. Am. Chem. Soc.* **1994**, *116*, 2064; e) J. F. Arenas, I. Lopez-Tocon, J. C. Otero, J. Soto, *J. Am. Chem. Soc.* **2002**, *124*, 1728.

[10] S. M. Lim, T. S. Kim, G. I. Lim, S. K. Kim, Y. S. Choi, *Chem. Phys. Lett.* **1998**, *288*, 828.

[11] Gaussian03W, full list of authors are available in supporting information.

[12] J. F. Stanton, J. Gauss, J. D. Watts, M. Nooijen, N. Oliphant, S. A. Perera, P. G. Szalay, S. J. Lauderdale, S. R. Gwaltney, S. Beck, A. Balkova, D. E. Berhholdt, K. K. Baeck, P. Rozyczko, H. Sekino, C. Hober, R. J. Bartlett, ACES-2, a product of the University of Florida, QuantumTheory Project.

[13] MolPro, H.-J. Werner, P. J. Knowles, R. Lindh, F. R. Manby, M. Schütz, P. Celani, T. Korona, A. Mitrushenkov, G. Rauhut, T. B. Adler, R. D. Amos, A. Bernhardsson, A. Berning, D. L. Cooper, M. J. O. Deegan, A. J. Dobbyn, F. Eckert, E. Goll, C. Hampel, G. Hetzer, T. Hrenar, G. Knizia, C. Köppl, Y. Liu, A. W. Lloyd, R. A. Mata, A. J. May, S. J. McNicholas, W. Meyer, M. E. Mura, A. Nicklaß, P. Palmieri, K. Pflüger, R. Pitzer, M. Reiher, U. Schumann, H. Stoll, A. J. Stone, R. Tarroni, T. Thorsteinsson, M. Wang, A. Wolf.

[14] a) A. Peluso, F. Santoro, G. D. Re, *Int. J. Quantum Chem.* **1997**, *63*, 233; b) R. Borrelli, A. Peluso, *J. Chem. Phys.* **2003**, *119*, 8437.